HHS Public Access

Author manuscript

Circ Cardiovasc Imaging. Author manuscript; available in PMC 2019 August 01.

Published in final edited form as:

Circ Cardiovasc Imaging. 2018 August ; 11(8): e007657. doi:10.1161/CIRCIMAGING.118.007657.

Coronary CTA-specific Definitions of High-Risk Plaque Features Improve Detection of ACS: Results from the ROMICAT II Trial

Daniel O. Bittner, MD[1,2,3], **Thomas Mayrhofer, PhD**[1,2,4], **Stefan B. Puchner, MD**[1,2,5], **Michael T. Lu, MD**[1,2], **Pal Maurovich-Horvat, MD, MPH**[6], **Khristine Ghemigian, BA, MHS**[1,2], **Pieter H. Kitslaar, MSc**[7,8], **Alexander Broersen, PhD**[7], **Fabian Bamberg, MD, MPH**[9], **Quynh A. Truong, MD, MPH**[10], **Christopher L. Schlett, MD, MPH**[11], **Udo Hoffmann, MD, MPH**[1,2], and **Maros Ferencik, MD, PhD**[1,2,12]

[1]Department of Radiology, Massachusetts General Hospital and Harvard Medical School, Boston, MA [2]Cardiac MR PET CT Program, Massachusetts General Hospital and Harvard Medical School, Boston, MA [3]Friedrich-Alexander University Erlangen-Nürnberg (FAU), Department of Cardiology, University Hospital Erlangen, Germany [4]School of Business Studies, Stralsund University of Applied Sciences, Stralsund, Germany [5]Department of Biomedical Imaging and Image-Guided Therapy, Medical University Vienna, Vienna, Austria [6]MTA-SE Lendület Cardiovascular Imaging Research Group, Heart and Vascular Centre, Semmelweis University, Budapest, Hungary [7]Department of Radiology, Division of Image Processing, Leiden University Medical Center, Leiden, the Netherlands [8]Medis medical imaging systems B.V, Leiden, the Netherlands [9]Department of Radiology, University of Tuebingen, Germany [10]Dalio Institute of Cardiovascular Imaging, New York-Presbyterian Hospital and Weill Cornell Medical College, New York, NY [11]Department of Diagnostic and Interventional Radiology, University Hospital Heidelberg, Heidelberg, Germany [12]Knight Cardiovascular Institute, Oregon Health and Science University, Portland, OR

Abstract

Background—High-risk plaque features (HRP) as detected by coronary CT angiography (CTA) predict acute coronary syndrome (ACS). We sought to determine whether coronary CTA-specific definitions of HRP improve discrimination of patients with ACS as compared to definitions from intravascular ultrasound (IVUS).

Methods and Results—In patients with suspected ACS, randomized to coronary CTA in the ROMICAT II trial, we retrospectively performed semi-automated quantitative analysis of HRP (including remodeling index, plaque burden as derived by plaque area, low CT attenuation plaque volume) and degree of luminal stenosis and analyzed the performance of traditional IVUS thresholds to detect ACS. Further, we derived CTA-specific thresholds in ACS patients to detect culprit lesions, and applied those to all patients to calculate the discriminatory ability to detect ACS in comparison to IVUS thresholds.

Corresponding author: Daniel Bittner, MD; Massachusetts General Hospital, Harvard Medical School and Department of Cardiology, University Hospital Erlangen, Friedrich-Alexander University Erlangen-Nürnberg (FAU), Germany; Phone: +49-9131-85-35301; Fax: +49-9131-85-35303; daniel.bittner@uk-erlangen.de.

Clinical Trial Registration Information: URL: https://clinicaltrials.gov. Unique identifier: NCT01084239

Out of 472 patients, 255 patients (56±7.8 years; 63% men) had coronary plaque. In 32 patients (6.8%) with ACS, culprit plaques (n=35) differed from non-culprit plaques (n=172) with significantly greater values for all HRP features except minimal luminal area (significantly lower) (all p<0.01). IVUS definitions showed good performance while minimal luminal area (OR: 6.82; p=0.014) and plaque burden (OR: 5.71, p=0.008) were independently associated with ACS, but not remodeling index (OR: 0.78; p=0.673). Optimized CTA-specific thresholds for plaque burden (AUC: 0.832 vs. 0.676) and degree of stenosis (AUC: 0.826 vs. 0.721) showed significantly higher diagnostic performance for ACS as compared to IVUS based thresholds (all p<0.05) with borderline significance for minimal luminal area (AUC: 0.817 vs. 0.742; p=0.066).

Conclusions—CTA-specific definitions of high-risk plaque features may improve the discrimination of patients with ACS as compared to IVUS based definitions.

Keywords

coronary CT angiography; acute coronary syndrome; acute chest pain; high-risk-plaque feature; culprit lesion; intravascular ultrasound

Subject Terms

Computerized Tomography (CT); Acute Coronary Syndromes; Coronary Artery Disease; Ultrasound; Imaging

Introduction

Morphologic characteristics of coronary plaques called high-risk plaque (HRP) features are associated with culprit lesion of ACS and provide incremental prognostic value over clinical risk factors and significant coronary artery stenosis[1–6]. In intravascular ultrasound (IVUS), the presence of thin-cap-fibroatheroma (TCFA)[7], minimal luminal area (MLA) ≤4.0 mm^2 [7–10], remodeling index (RI) >1.05[11, 12] and plaque burden ≥70%[7] are frequently used thresholds to identify coronary plaque associated with increased risk for cardiovascular events[7, 13, 14].

Coronary computed tomography angiography (CTA) is a reasonable modality to approach patients with suspected acute coronary syndrome (ACS)[15–17], due to its high accuracy to detect coronary artery stenosis and its ability to visualize atherosclerosis[18–20]. Moreover, coronary CTA provides detailed information about plaque morphology and composition[1–3, 21], and may become the main diagnostic tool for non-invasive plaque characterization.

Spatial and temporal resolution, and ability for tissue characterization of coronary CTA and IVUS differ significantly. However, specific definitions for HRP do not exist for coronary CTA and definitions from IVUS have been used previously. In coronary CTA, plaque characteristics can be assessed not only qualitatively but also quantitatively, which has been validated extensively against IVUS[5, 22–24]. Novel software applications now permit (semi-) automated assessment and quantification of coronary plaque, which has been shown to be feasible[25] and valuable[26].

The performance of IVUS definitions for HRP features detected by coronary CTA is unknown and independently derived thresholds of HRP feature from coronary CTA are not available. Therefore, we performed CTA-based quantitative analyses in patients presenting with acute chest pain and sought to derive optimized CTA-specific definitions of HRP features for the prediction of ACS. We tested whether there was a difference between IVUS-based and CTA-specific thresholds and whether CTA-specific HRP definitions improved the discrimination of patients with ACS.

Materials and Methods

Study design and patient population

The study cohort consisted of patients from the Rule Out Myocardial Infarction/Ischemia Using Computer Assisted Tomography (ROMICAT) II trial. Individuals, who were randomly assigned to the coronary CTA arm and underwent CTA, were included in this analysis. A detailed description of the patient population was previously reported[15].

In summary, this multicenter trial (nine sites in the US) enrolled 1000 patients with acute chest pain and clinical suspicion for ACS presenting to the ED between April 2010 and January 2012. Enrolment criteria were: 40-74 years of age, negative initial cardiac troponin and electrocardiogram without ischemic changes. All study participants provided written informed consent for participation in the ROMICAT II trial and the local institutional review boards approved the study.

CT image acquisition and analysis

For the acquisition of coronary CTA images either retrospectively ECG-gated or prospectively ECG-triggered protocols were used with at least 64-mutidetector row CT technology. Each data set was analyzed by one of four readers with at least 5 years of experience and level III training in coronary CTA. Quantitative plaque analysis was performed using a dedicated workstation and coronary plaque analysis software (QAngio CT RE 2.0, Medis medical imaging systems b.v., Leiden, the Netherlands). Datasets were randomly assigned in equal parts to all four readers. All readers analyzed 20 randomly selected coronary CTA datasets to calculate inter-observer variability.

The quantitative plaque analysis was performed on coronary segment basis, in all segments with visually detectable plaques. Segments with image quality graded as non-diagnostic were excluded from the analysis (n=108/3,804). The readers followed a stepwise procedure as displayed in Figure 1 and Supplemental Figures 1–5: 1. Major coronary arteries were automatically identified, 2. Luminal and outer vessel boundaries were automatically delineated by the software, 3. The readers performed manual adjustments of boundaries if necessary, 4. The proximal and distal end of the coronary plaque was chosen where normal artery could be identified at the proximal and distal site or at the beginning and end of the coronary segment if no normal artery was identified in the segment.

All measurements were exported to an Excel file. Measurements performed at segments level were: diameter stenosis (calculated as the ratio of the minimal luminal diameter in the coronary segment and the average of the luminal diameter at the proximal and distal

references), minimal luminal area (MLA=luminal area at the site of maximum stenosis), plaque burden (calculated as plaque area divided by outer vessel area at the site of maximum stenosis), coronary plaque volume, plaque volume of subcomponents at <30 HU and <60 HU, lesion length (calculated as the centerline distance from the proximal to distal end of the plaque, remodeling index (calculated as the ratio of the outer vessel wall area at the site of the MLA and the vessel area defined by the vessel wall reference at that location). We also calculated relative plaque volume of low HU plaque at <30 HU and <60 HU, defined as the ratio between the volume of plaque subcomponents at <30HU or <60HU and the volume of the entire plaque.

Detection of culprit plaque

We detected culprit coronary plaque in patients with diagnosis of ACS during the index hospitalization. The diagnosis of ACS (acute myocardial infarction or unstable angina pectoris) was determined by an external, independent clinical end-point committee according to the ACC/AHA guidelines and was previously described[15]. To identify the culprit lesions in patients with ACS, an independent investigator, reviewed all available clinical data and reports, including additional cardiac testing (e.g. ICA, stress echocardiograms, nuclear myocardial perfusion stress tests). The primary decision on the location of culprit lesions was made on the basis of ICA reports. ICA was performed in 32 out of 37 patients with ACS. We assigned the culprit lesion to coronary segments, in which percutaneous coronary intervention was performed. In patients who underwent coronary artery by-pass grafting (n=4), we assigned culprit lesions to all segments with ≥70% stenosis or ≥50% stenosis for the left main coronary artery. Six patients underwent ICA without revascularization. The culprit lesion in those patients was assigned to the coronary segment with the highest degree of diameter stenosis on ICA. Patients not undergoing ICA (n=5) were excluded from this analysis, as the culprit lesion could not be clearly defined.

Analysis of HRP feature definitions

We performed a per segment analysis, to determine the CTA-based quantitative plaque measurements that are associated with culprit lesions in ACS patients. In each ACS patient, we analyzed each plaque feature for each segment with plaque (minimal luminal area, remodeling index, plaque burden, lesion length, absolute and relative plaque volume of low HU plaque at <30 HU and <60 HU and diameter stenosis). The results were reported at segment level. To determine differences in quantitative plaque measurements we compared culprit plaque to all non-culprit plaques in patients with ACS.

For the diagnostic performance analysis of traditional IVUS thresholds for HRP features to detect patients with ACS, we used minimal luminal area ≤4.0 mm^2 [7–10], remodeling index >1.05[11, 12] and remodeling index >1.1, plaque burden ≥70%[7], lesion length 11.2 mm[7] and volume of plaque <30HU attenuation as TCFA equivalent, as low attenuation plaque <30HU was shown to qualitatively correspond to a lipid rich necrotic core on coronary CTA[5, 21–23]. For the volume of low HU plaque, we used a derived, CTA-specific threshold of 1.31mm^3, as there is no equivalent definition based on IVUS. Thresholds from invasive angiography were used for diameter stenosis (≥50% or ≥70%).

To derive optimized CTA-specific HRP definitions, we used receiver operating characteristic curves (ROC) of plaque measures to identify the maximum of the sum for sensitivity and specificity to discriminate culprit plaque from non-culprit plaque. Culprit plaque-based thresholds were then applied to all patients (with and without ACS) to identify the presence of any plaque feature above the respective culprit plaque-based thresholds on per patient basis and subsequently calculate the diagnostic performance for the detection of ACS. Diagnostic performance of the newly derived thresholds was then compared to above-mentioned traditional thresholds from IVUS in a dichotomized fashion.

Statistical Analysis

Continuous data are presented as mean ± standard deviation or median with 25th and 75th percentile, and categorical or ordinal variables are presented as absolute and relative frequencies. On a per patient level, comparisons between groups were performed with an independent student t-test or the Wilcoxon rank-sum test for continuous variables, Fisher's exact test for categorical variables, and Wilcoxon rank-sum test for ordinal variables. On a segmental level, comparisons between groups were performed using univariable multilevel mixed-effects logistic regression models that account for the group structure (i.e. multiple segments per patient) and thus possible autocorrelation effects in the data. To evaluate interobserver agreement among four readers, intraclass correlation coefficient (ICC) was calculated using two-way random-effects models. To determine co-linearities among all HRP features, we assessed Spearman's rank correlation coefficients. Uni- and multivariable multilevel mixed-effects logistic regression analysis were performed to identify determinants for culprit lesion within ACS patients and determinants for ACS among all patients. In the multivariable model we included remodeling index, minimal luminal area (mm^2), plaque burden (%), TCFA equivalent – Low HU plaque volume <30 HU (mm^3) and lesion length. The discriminatory capacity of the dichotomized HRP thresholds for the prediction of culprit lesion and ACS was assessed using the area under curve (AUC)[27]. Multivariable logistic regression models were used to calculate receiver operating characteristic (ROC) curves. A two-tailed p-value of <0.05 was considered statistically significant. All statistical analyses were performed using Stata 13.1 (Stata- Corp LP, College Station, Texas). The complete source data from the Rule Out Myocardial Infarction/Ischemia Using Computer Assisted Tomography (ROMICAT) II trial are publicly available in accordance with the data sharing policy of the National Institutes of Health and can be used for the purposes of reproducing the results or replicating the procedures.

Results

Study population

In the ROMICAT II trial, 501 patients were randomly assigned to the coronary CTA arm of the study and 472 of them underwent coronary CTA as the first test. Quantitative plaque analysis was performed in 255 patients (mean age 56±7.8 years; 62.7% men), in whom coronary artery plaque was visually identified. ACS was diagnosed in 32 (6.8%) patients (myocardial infarction n=5, unstable angina pectoris n=32), 203 patients were adjudicated as non-cardiac chest pain, 3 as non-coronary cardiac chest pain and 17 as cardiac chest pain not meeting ACS criteria. Baseline characteristics are summarized in Table 1.

Inter-observer variability of quantitative coronary plaque analysis

Among four readers, the segment-based inter-observer agreement for the quantitative measurements ranged from good to very good. Correlation for each measurement was as follows: ICC 0.69 (95%CI 0.60 to 0.77) for remodeling index, ICC 0.97 (95%CI 0.96 to 0.98) for minimal luminal area, ICC 0.92 (95%CI 0.89 to 0.94) for plaque burden, ICC 0.80 (95%CI 0.74 to 0.86) for volume of plaque with <30HU, ICC 0.95 (95%CI 0.93 to 0.96) for diameter stenosis and ICC 0.98 (95%CI 0.98 to 0.99) for lesion length.

Association of HRP characteristics with culprit plaques of ACS

We identified 35 culprit plaques and 172 non-culprit plaques in 32 patients with ACS based on clinical information including ICA results. Differences among mean HU-specific plaque volumes was highest for volume of plaque <30 HU comparing culprit and non-culprit plaque (2.34 vs. 0.19 mm^3; p<0.001). Therefore, plaque attenuation <30HU was used to represent TCFA in our analysis (Supplemental Table 1). All remaining HRP characteristics, assessed as continuous measures, also showed significant differences between culprit and non-culprit plaques as summarized in Table 2 (all p<0.01).

To determine which HRP features are associated with ACS using IVUS definitions, we used pre-specified dichotomized IVUS thresholds for this analysis. We found that all HRP features, exept remodling index, were significantly associated with culprit plaques in a univariable analysis among 207 coronary plaques within 32 ACS patients, as summarized in Table 3a. In a multivariable model, we found independent associations only for dichotomized thresholds of low HU plaque volume (OR 6.60 (95%CI 2.52-17.24; p<0.001)) and plaque burden (OR 3.14 (95%CI 1.06-9.25); p=0.038)). Using a predefined remodeling index of 1.05 instead of 1.10 as above showed similar results (Supplemental Table 2A).

We also found close correlations among HRP features, as listed in Supplemental Table 3. In brief, MLA showed the strongest inverse correlation with plaque burden with a Spearman's correlation coefficient (CC) of −0.81, followed by diameter stenosis (CC: −0.73), lesion length (CC: −0.53) and TCFA equivalent (<30 HU plaque volume) (CC: −0.31).

Association of traditional HRP definitions (IVUS) with ACS

On a patient level, using dichotomized IVUS thresholds, MLA, plaque burden, lesion length and low HU plaque volume were independently associated to ACS as displayed in Table 3b, but not remodeling index (OR 0.78 (95%CI 0.25-2.45; p=0.673)). Similar results were found using a remodeling index of 1.05 instead of 1.10 (Supplemental Table 2B).

The overall diagnostic performance of dichotomized IVUS thresholds ranged from good to very good (Table 4). The probability of ACS associated with the presence of plaque that were characterized as low HU (TCFA equivalent) increased according to the additional presence of plaque burden ≥70% and MLA ≤4.0 mm^2, from 25.3% to 69.9.0% respectively (Figure 2). The presence of plaque burden ≥70% (AUC: 0.791 (95%CI 0.711-0.872)) and MLA≤4.0 mm^2 (AUC: 0.865 (95%CI 0.792-0.919)) was associated with higher discriminatory capacity to detect ACS beyond TCFA equivalent (AUC: 0.725 (95%CI 0.652-0.800)), as displayed in Figure 3 (p=0.0082 and p=0.0190 respectively).

HRP definitions optimized for coronary CTA in comparison to IVUS-based thresholds

Optimized quantitative HRP definitions for coronary CTA showed the maximum of the sum of sensitivity and specificity for the following thresholds: 1.17 for remodeling index, 1.43 mm^2 for MLA, 55% for plaque burden, 1.31 mm^3 for low HU plaque volume, 52% for diameter stenosis and 13.09 mm for lesion length.

The diagnostic performance of new derived thresholds was high as listed in Table 4 (more details in Supplemental Table 4). Compared to traditional IVUS thresholds, optimized thresholds showed significantly higher diagnostic performance for plaque burden (AUC: 0.832 (95%CI (0.768-0.896) vs. 0.676 (95%CI (0.591-0.762); p<0.001) and borderline significant for MLA (AUC: 0.817 (95%CI (0.736-0.898) vs. 0.742 (95%CI (0.689-0.796); p=0.066) but not for remodeling index and lesion length. There was also a significant difference in diameter stenosis using the optimized threshold of 52% as compared to ≥70% (AUC: 0.826 (95%CI (0.743-0.908) vs. 0.721 (95%CI 0.721 (0.632-0.810); p=0.005). Overall high discriminatory capacity was also seen for the threshold of low HU plaque volume (AUC: 0.725 (95%CI (0.646-0.804)).

The above mentioned higher discriminatory capacity of the new derived thresholds for plaque burden and diameter stenosis translated into a significant improvement of the net reclassification index as shown in Table 4.

The presence of multiple HRP features in one patient (low HU plaque volume, MLA and plaque burden), showed high discriminatory capacity to detect ACS, using dichotomous pre-specified IVUS definitions as well as optimized CTA-specific definitions (AUC: 0.856 (95%CI 0.792-0.919)) vs. 0.900 (95%CI 0.824-0.956); p=0.235). Using all available information from quantitative coronary CTA assessment (low density plaque, MLA, plaque burden, RI, diameter stenosis and lesion length), optimized CTA definitions showed an increase in the diagnostic performance (AUC: 0.856 (95%CI 0.792-0.919) vs. 0.932 (95%CI 0.859 - 0.979); p=0.021) as visualized in Figure 4.

Discussion

Our study confirmed previous observations of differences in atherosclerotic plaque characteristics between culprit and non-culprit plaques. We demonstrated that HRP thresholds based on IVUS definitions had adequate performance to detect ACS using quantitative plaque analysis in coronary CTA. Moreover, this is the first multicenter study that independently derived optimized coronary CTA-specific HRP definitions, demonstrating significant differences and higher accuracy to traditional IVUS-based definitions.

Diagnostic performance of IVUS-based thresholds in coronary CTA

The prospective natural-history study of coronary atherosclerosis (PROSPECT)[7] demonstrated that minimal luminal area and plaque burden, as detected by IVUS, were amongst the strongest predictors for future major cardiovascular events in previously not culprit plaque. In IVUS, MLA equal or below 4.0 mm^2 and plaque burden equal or above 70.0% were associated with an over 3-fold and 5-fold increased risk for future events respectively (both p<0.001). We demonstrated similar strength of association with ACS in

our study. MLA was associated with almost 7-fold and plaque burden with almost 6-fold increased risk of ACS using IVUS-based thresholds for quantitative coronary CTA analysis. In addition, we saw incremental value of these dichotomous thresholds beyond the presence of plaque that was characterized as low HU (TCFA equivalent) in coronary CTA.

In contrast, remodeling index was found to be the weakest predictor of ACS in our analysis. In a multivariate model, it was neither independent nor incremental in the detection of ACS, potentially due to existing co-linearities with other HRP features. Notably, this is in line with results from the PROSPECT trial[7], where remodeling index was also not an independent determinant for future cardiac events.

Comparison of traditional IVUS and coronary CTA derived thresholds

Similar to IVUS, optimized CTA definitions for MLA and plaque burden showed the strongest association to ACS in our analysis. However, differences in quantitative thresholds exist. In particular, the diagnostic performance of plaque burden was significantly higher using a threshold of 55% vs. the IVUS threshold of 70% ($p<0.001$). This finding is in line with data from Versteylen and colleagues[26]. In this retrospective analysis, including 25 patients with ACS and 101 controls, who underwent coronary CTA and semi-automated plaque quantification, a plaque burden of 45% provided the highest sum of sensitivity and specificity. The lower spatial resolution of CT and subsequent underestimation of noncalcified plaque volume in coronary CT might account for this discrepancy[28].

As mentioned before, a MLA of 4.0 mm^2 or less was associated with a significantly higher likelihood for recurrent events in IVUS (HR: 3.21, $p=0.001$)[7] and in patients with lesions above 4.0 mm^2, intervention could be deferred safely[8]. In contrast, for coronary CTA a threshold of 1.43 mm^2 showed a borderline significant higher diagnostic performance ($p=0.066$) to discriminate patients with ACS. Our result is similar to the cut-off found in a recently published prospective analysis of 160 patients, in which a MLA ≤1.8 mm^2 in coronary CTA was shown to be most accurate for the prediction of hemodynamically significant stenosis by ICA and FFR[29]. Technical requirements may potentially explain discrepancies between CTA and IVUS, as IVUS is usually limited to proximal and middle portions of epicardial vessels, but no restrictions were applied to coronary CTA data sets in our study, except exclusions due to non-diagnostic image quality (below 3%). Due to the ability to determine MLA even in peripheral vessels and side branches using coronary CT plaque quantification, the reference vessel area at the site of each individual lesion of interest has to be to be taken into account. As the here proposed optimized threshold of 1.43 mm^2 can certainly not be used individually for patients with e.g. left main or proximal LAD disease, indicates the need for more granular information in respect to valid minimal luminal area reference values also for medium and small vessels. Whether indexing the lesion specific MLA to the reference vessel might be an adequate solution to address this aspect, will need to be tested in future analysis.

In addition, above-mentioned IVUS data demonstrated the association of MLA with mid and long-term risk for subsequent cardiovascular events in previously non-culprit lesions, while the underlying quantitative coronary CTA assessment aimed to optimize HRP definitions for the immediate diagnosis of ACS according to culprit lesions. MLA was consistent with

degree of stenosis in our analysis and as the diagnosis of ACS was predominately driven by obstructive CAD in this acute chest pain cohort, MLA might therefore differ from the traditional threshold.

Thin-cap fibroatheroma, as detected by IVUS, has been also shown to be a strong predictor of future cardiovascular events[7]. Qualitatively, low HU plaque (<30HU) and Napkin-Ring Sign (NRS) correspond to a lipid rich necrotic core in coronary CTA[5, 21–23]. Beyond that, we could now demonstrate, that quantitative assessment of low HU plaque volume, is not only independently associated with culprit plaque in ACS patients, but also with ACS among all patients with coronary plaque. The volume threshold of 1.31 mm^3 provides good sensitivity, high negative predictive value (96%) and good diagnostic accuracy to discriminate patients with ACS from those without ACS. Thus, this CTA-specific definition seems to be a reasonable threshold for quantitative plaque analysis and adds more granular information beyond the attenuation threshold of 30HU. This might be useful, as coronary CTA is already a viable modality to approach patients with suspected ACS[15–17] and may become the main non-invasive diagnostic test for the assessment of HRP features.

New CTA-based measures of high-risk plaque

One plaque characteristic that has been paid little attention to in coronary CTA so far is lesion length, which has previously not only been shown to differ between ACS and non ACS patients[6], but also to be a strong determinant of hemodynamic relevant stenosis[30] improving the correlation of functional assessment and anatomic severity as demonstrated by fractional flow reserve[31]. In fact, our analysis showed that lesion length was significantly higher in culprit plaque as compared to non-culprit plaque ($p<0.001$) and was independently associated with ACS in patients with coronary plaque. This translated to a good diagnostic performance (AUC: 0.8) for this individual HRP feature. A potential explanation for the independent value of lesion length is that very few HRP features account for longitudinal plaque dimensions.

This data suggests, that the use of all available quantitative plaque information provided by coronary CTA, including lesion length, may further improve the detection of ACS and should therefore be considered in future analysis to better allow for determining its clinical value in prospective studies.

Limitations

Some limitations of this study need to be mentioned. First, quantitative coronary plaque assessment is time consuming and requires substantial readers expertise, albeit a semi-automated software was used. Improvements in software algorithm are needed to further facilitate measurements and demonstrate feasibility for the use in clinical routine. Second, due to a limited incidence of disease (ACS: n=37), small differences in definitions for HRP features might not be apparent, even though the overall number of patient included in this analysis was substantial. Third, in this cohort we focused on the immediate diagnosis of ACS for the derivation of coronary CTA specific HRP definitions. Although IVUS definitions in PRSOPECT trial were used to predict future events, very similar definitions were also shown to be present in patients with immediate diagnosis of acute coronary

syndrome[32]. Validation of these new definitions will be necessary in an independent cohort and we further need to determine whether these can also improve mid- and long-term prediction of ACS and major adverse cardiovascular events.

Conclusion

Marked differences in plaque extent and morphology are present comparing culprit and non-culprit plaques in patients experiencing ACS. We could demonstrate significant differences and higher accuracy of independently derived optimized coronary CTA-specific HRP definitions, suggesting improvement in discrimination of patients with ASC, as compared to traditional IVUS-based definitions.

Supplementary Material

Refer to Web version on PubMed Central for supplementary material.

Acknowledgments

Sources of Funding

This work was supported by grants from the National Heart, Lung, and Blood Institute (U01HL092040 and U01HL092022). Dr. Bittner and Dr. Mayrhofer were supported by NIH/NHLBI 5K24HL113128. Dr. Truong received support from the NIH/NHLBI K23HL098370 and L30HL093896. Dr. Ferencik received support from the American Heart Association (13FTF16450001).

Disclosures:

Pieter H. Kitslaar is an employee of Medis medical imaging systems B.V. Dr. Truong received grant support from Qi Imaging LLC, and was consultant to American College of Radiology, Society of Cardiovascular Computed Tomography, and Aralez Pharmaceuticals. Dr. Hoffmann received research grant support from Siemens Medical Solutions and Heart Flow Inc. and consultant/advisory board support from Heart Flow Inc.

References

1. Motoyama S, Sarai M, Harigaya H, Anno H, Inoue K, Hara T, Naruse H, Ishii J, Hishida H, Wong ND, Virmani R, Kondo T, Ozaki Y, Narula J. Computed tomographic angiography characteristics of atherosclerotic plaques subsequently resulting in acute coronary syndrome. J Am Coll Cardiol. 2009; 54:49–57. [PubMed: 19555840]
2. Hoffmann U, Moselewski F, Nieman K, Jang IK, Ferencik M, Rahman AM, Cury RC, Abbara S, Joneidi-Jafari H, Achenbach S, Brady TJ. Noninvasive assessment of plaque morphology and composition in culprit and stable lesions in acute coronary syndrome and stable lesions in stable angina by multidetector computed tomography. J Am Coll Cardiol. 2006; 47:1655–62. [PubMed: 16631006]
3. Puchner SB, Liu T, Mayrhofer T, Truong QA, Lee H, Fleg JL, Nagurney JT, Udelson JE, Hoffmann U, Ferencik M. High-risk plaque detected on coronary CT angiography predicts acute coronary syndromes independent of significant stenosis in acute chest pain: results from the ROMICAT-II trial. J Am Coll Cardiol. 2014; 64:684–92. [PubMed: 25125300]
4. Pflederer T, Marwan M, Schepis T, Ropers D, Seltmann M, Muschiol G, Daniel WG, Achenbach S. Characterization of culprit lesions in acute coronary syndromes using coronary dual-source CT angiography. Atherosclerosis. 2010; 211:437–44. [PubMed: 20189568]
5. Maurovich-Horvat P, Ferencik M, Voros S, Merkely B, Hoffmann U. Comprehensive plaque assessment by coronary CT angiography. Nat Rev Cardiol. 2014; 11:390–402. [PubMed: 24755916]
6. Ferencik M, Schlett CL, Ghoshhajra BB, Kriegel MF, Joshi SB, Maurovich-Horvat P, Rogers IS, Banerji D, Bamberg F, Truong QA, Brady TJ, Nagurney JT, Hoffmann U. A computed tomography-

based coronary lesion score to predict acute coronary syndrome among patients with acute chest pain and significant coronary stenosis on coronary computed tomographic angiogram. Am J Cardiol. 2012; 110:183–9. [PubMed: 22481015]

7. Stone GW, Maehara A, Lansky AJ, de Bruyne B, Cristea E, Mintz GS, Mehran R, McPherson J, Farhat N, Marso SP, Parise H, Templin B, White R, Zhang Z, Serruys PW, Investigators P. A prospective natural-history study of coronary atherosclerosis. N Engl J Med. 2011; 364:226–35. [PubMed: 21247313]
8. Abizaid AS, Mintz GS, Mehran R, Abizaid A, Lansky AJ, Pichard AD, Satler LF, Wu H, Pappas C, Kent KM, Leon MB. Long-term follow-up after percutaneous transluminal coronary angioplasty was not performed based on intravascular ultrasound findings: importance of lumen dimensions. Circulation. 1999; 100:256–61. [PubMed: 10411849]
9. Abizaid A, Mintz GS, Pichard AD, Kent KM, Satler LF, Walsh CL, Popma JJ, Leon MB. Clinical, intravascular ultrasound, and quantitative angiographic determinants of the coronary flow reserve before and after percutaneous transluminal coronary angioplasty. Am J Cardiol. 1998; 82:423–8. [PubMed: 9723627]
10. Nishioka T, Amanullah AM, Luo H, Berglund H, Kim CJ, Nagai T, Hakamata N, Katsushika S, Uehata A, Takase B, Isojima K, Berman DS, Siegel RJ. Clinical validation of intravascular ultrasound imaging for assessment of coronary stenosis severity: comparison with stress myocardial perfusion imaging. J Am Coll Cardiol. 1999; 33:1870–8. [PubMed: 10362187]
11. Pasterkamp G, Borst C, Gussenhoven EJ, Mali WP, Post MJ, The SH, Reekers JA, van den Berg FG. Remodeling of De Novo atherosclerotic lesions in femoral arteries: impact on mechanism of balloon angioplasty. J Am Coll Cardiol. 1995; 26:422–8. [PubMed: 7608445]
12. Schoenhagen P, Ziada KM, Kapadia SR, Crowe TD, Nissen SE, Tuzcu EM. Extent and direction of arterial remodeling in stable versus unstable coronary syndromes: an intravascular ultrasound study. Circulation. 2000; 101:598–603. [PubMed: 10673250]
13. Little WC, Constantinescu M, Applegate RJ, Kutcher MA, Burrows MT, Kahl FR, Santamore WP. Can coronary angiography predict the site of a subsequent myocardial infarction in patients with mild-to-moderate coronary artery disease? Circulation. 1988; 78:1157–66. [PubMed: 3180375]
14. Varnava AM, Mills PG, Davies MJ. Relationship between coronary artery remodeling and plaque vulnerability. Circulation. 2002; 105:939–43. [PubMed: 11864922]
15. Hoffmann U, Truong QA, Schoenfeld DA, Chou ET, Woodard PK, Nagurney JT, Pope JH, Hauser TH, White CS, Weiner SG, Kalanjian S, Mullins ME, Mikati I, Peacock WF, Zakroysky P, Hayden D, Goehler A, Lee H, Gazelle GS, Wiviott SD, Fleg JL, Udelson JE, Investigators R-I. Coronary CT angiography versus standard evaluation in acute chest pain. N Engl J Med. 2012; 367:299–308. [PubMed: 22830462]
16. Goldstein JA, Chinnaiyan KM, Abidov A, Achenbach S, Berman DS, Hayes SW, Hoffmann U, Lesser JR, Mikati IA, O'Neil BJ, Shaw LJ, Shen MY, Valeti US, Raff GL, Investigators C-S. The CT-STAT (Coronary Computed Tomographic Angiography for Systematic Triage of Acute Chest Pain Patients to Treatment) trial. J Am Coll Cardiol. 2011; 58:1414–22. [PubMed: 21939822]
17. Litt HI, Gatsonis C, Snyder B, Singh H, Miller CD, Entrikin DW, Leaming JM, Gavin LJ, Pacella CB, Hollander JE. CT angiography for safe discharge of patients with possible acute coronary syndromes. N Engl J Med. 2012; 366:1393–403. [PubMed: 22449295]
18. Meijboom WB, Meijs MF, Schuijf JD, Cramer MJ, Mollet NR, van Mieghem CA, Nieman K, van Werkhoven JM, Pundziute G, Weustink AC, de Vos AM, Pugliese F, Rensing B, Jukema JW, Bax JJ, Prokop M, Doevendans PA, Hunink MG, Krestin GP, de Feyter PJ. Diagnostic accuracy of 64-slice computed tomography coronary angiography: a prospective, multicenter, multivendor study. J Am Coll Cardiol. 2008; 52:2135–44. [PubMed: 19095130]
19. Miller JM, Rochitte CE, Dewey M, Arbab-Zadeh A, Niinuma H, Gottlieb I, Paul N, Clouse ME, Shapiro EP, Hoe J, Lardo AC, Bush DE, de Roos A, Cox C, Brinker J, Lima JA. Diagnostic performance of coronary angiography by 64-row CT. N Engl J Med. 2008; 359:2324–36. [PubMed: 19038879]
20. Achenbach S, Moselewski F, Ropers D, Ferencik M, Hoffmann U, MacNeill B, Pohle K, Baum U, Anders K, Jang IK, Daniel WG, Brady TJ. Detection of calcified and noncalcified coronary atherosclerotic plaque by contrast-enhanced, submillimeter multidetector spiral computed

tomography: a segment-based comparison with intravascular ultrasound. Circulation. 2004; 109:14–7. [PubMed: 14691045]

21. Kashiwagi M, Tanaka A, Kitabata H, Tsujioka H, Kataiwa H, Komukai K, Tanimoto T, Takemoto K, Takarada S, Kubo T, Hirata K, Nakamura N, Mizukoshi M, Imanishi T, Akasaka T. Feasibility of noninvasive assessment of thin-cap fibroatheroma by multidetector computed tomography. JACC Cardiovasc Imaging. 2009; 2:1412–9. [PubMed: 20083077]
22. Schlett CL, Maurovich-Horvat P, Ferencik M, Alkadhi H, Stolzmann P, Scheffel H, Seifarth H, Nakano M, Do S, Vorpahl M, Kauczor HU, Bamberg F, Tearney GJ, Virmani R, Hoffmann U. Histogram analysis of lipid-core plaques in coronary computed tomographic angiography: ex vivo validation against histology. Invest Radiol. 2013; 48:646–53. [PubMed: 23614976]
23. Marwan M, Taher MA, El Meniawy K, Awadallah H, Pflederer T, Schuhback A, Ropers D, Daniel WG, Achenbach S. In vivo CT detection of lipid-rich coronary artery atherosclerotic plaques using quantitative histogram analysis: a head to head comparison with IVUS. Atherosclerosis. 2011; 215:110–5. [PubMed: 21227419]
24. Voros S, Rinehart S, Qian Z, Joshi P, Vazquez G, Fischer C, Belur P, Hulten E, Villines TC. Coronary atherosclerosis imaging by coronary CT angiography: current status, correlation with intravascular interrogation and meta-analysis. JACC Cardiovasc Imaging. 2011; 4:537–48. [PubMed: 21565743]
25. Boogers MJ, Broersen A, van Velzen JE, de Graaf FR, El-Naggar HM, Kitslaar PH, Dijkstra J, Delgado V, Boersma E, de Roos A, Schuijf JD, Schalij MJ, Reiber JH, Bax JJ, Jukema JW. Automated quantification of coronary plaque with computed tomography: comparison with intravascular ultrasound using a dedicated registration algorithm for fusion-based quantification. Eur Heart J. 2012; 33:1007–16. [PubMed: 22285583]
26. Versteylen MO, Kietselaer BL, Dagnelie PC, Joosen IA, Dedic A, Raaijmakers RH, Wildberger JE, Nieman K, Crijns HJ, Niessen WJ, Daemen MJ, Hofstra L. Additive value of semiautomated quantification of coronary artery disease using cardiac computed tomographic angiography to predict future acute coronary syndrome. J Am Coll Cardiol. 2013; 61:2296–305. [PubMed: 23562925]
27. DeLong ER, DeLong DM, Clarke-Pearson DL. Comparing the areas under two or more correlated receiver operating characteristic curves: a nonparametric approach. Biometrics. 1988; 44:837–45. [PubMed: 3203132]
28. Leber AW, Becker A, Knez A, von Ziegler F, Sirol M, Nikolaou K, Ohnesorge B, Fayad ZA, Becker CR, Reiser M, Steinbeck G, Boekstegers P. Accuracy of 64-slice computed tomography to classify and quantify plaque volumes in the proximal coronary system: a comparative study using intravascular ultrasound. J Am Coll Cardiol. 2006; 47:672–7. [PubMed: 16458154]
29. Plank F, Burghard P, Friedrich G, Dichtl W, Mayr A, Klauser A, Wolf F, Feuchtner G. Quantitative coronary CT angiography: absolute lumen sizing rather than %stenosis predicts hemodynamically relevant stenosis. Eur Radiol. 2016; 26:3781–3789. [PubMed: 26863897]
30. Kristensen TS, Engstrom T, Kelbaek H, von der Recke P, Nielsen MB, Kofoed KF. Correlation between coronary computed tomographic angiography and fractional flow reserve. Int J Cardiol. 2010; 144:200–5. [PubMed: 19427706]
31. Brosh D, Higano ST, Lennon RJ, Holmes DR Jr, Lerman A. Effect of lesion length on fractional flow reserve in intermediate coronary lesions. Am Heart J. 2005; 150:338–43. [PubMed: 16086940]
32. Hong MK, Mintz GS, Lee CW, Suh J, Kim JH, Park DW, Lee SW, Kim YH, Cheong SS, Kim JJ, Park SW, Park SJ. Comparison of virtual histology to intravascular ultrasound of culprit coronary lesions in acute coronary syndrome and target coronary lesions in stable angina pectoris. Am J Cardiol. 2007; 100:953–9. [PubMed: 17826376]

Clinical Perspective

Marked differences in plaque extent and morphology can be detected in culprit as compared to non-culprit plaques by coronary CT angiography in patients with acute coronary syndrome. In our analysis, we found that the presence of high-risk plaque features (HRP) based on intra vascular ultrasound definitions had good diagnostic accuracy for the detection of ACS. However, we demonstrated significant differences and higher accuracy of independently derived optimized coronary CTA-specific HRP definitions, suggesting improvement in discrimination of patients with ACS as compared to traditional IVUS-based definitions. Prospective studies are needed to determine whether the use of all available quantitative plaque information provided by coronary CTA may improve the detection of ACS and subsequently add value in clinical care.

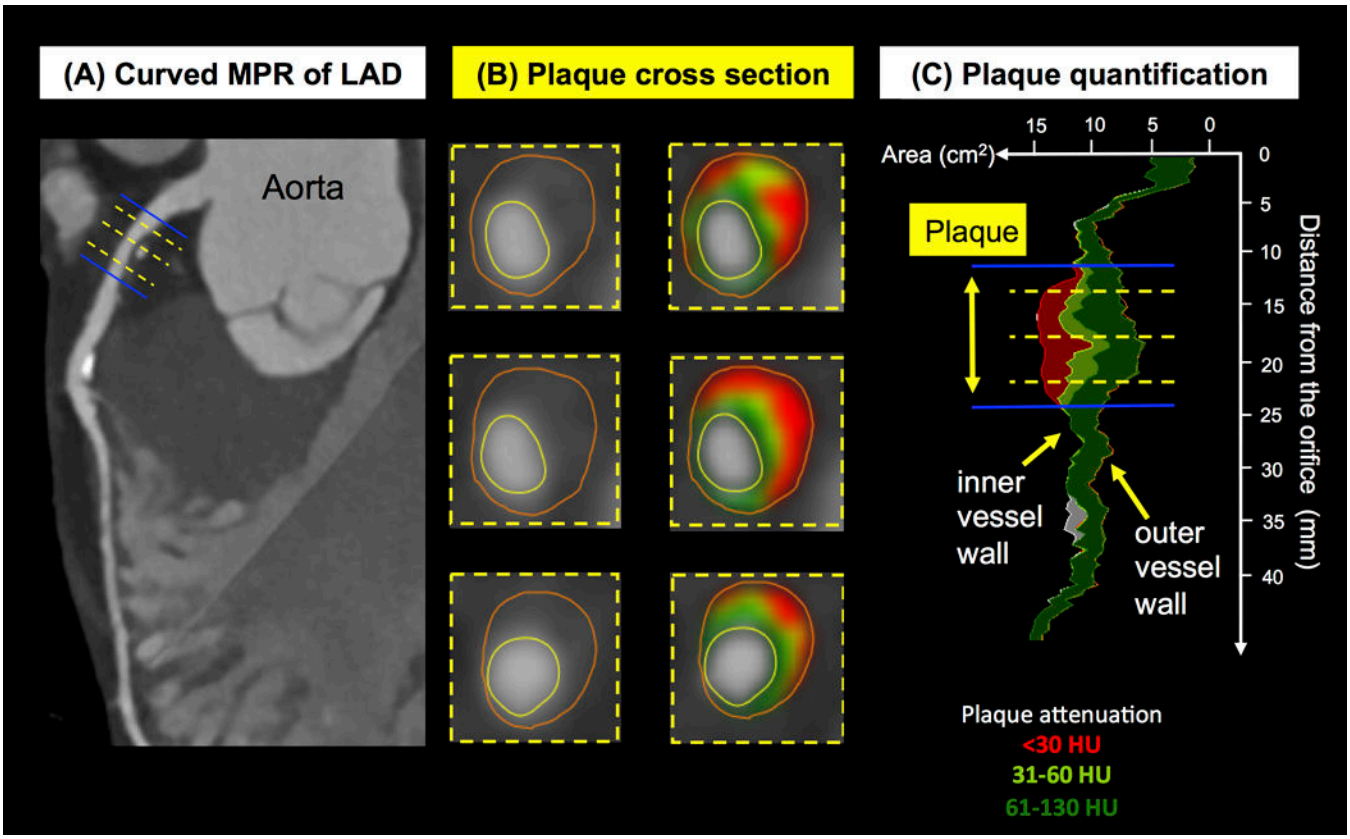

Figure 1. Stepwise measurements for quantitative plaque assessment using (semi-) automated software

Quantitative plaque measurements using semi-automated software. In a curved multiplanar reconstruction (MPR) of the left anterior descending (LAD) coronary artery in long axis (Figure A), the reader manually selects the beginning and end of the plaque (blue lines). The yellow lines indicate sites of the vessel cross-section displayed in Figure B. The software automatically delineates inner and outer vessel wall and detects plaque components with low CT attenuation <30HU (red), 31 to 60HU (light green) and 61 to 130HU (dark green). The software then provides stenosis degree, remodeling index, minimal luminal area, plaque burden and volumes of plaque and volumes of plaque subcomponents (Figure C).

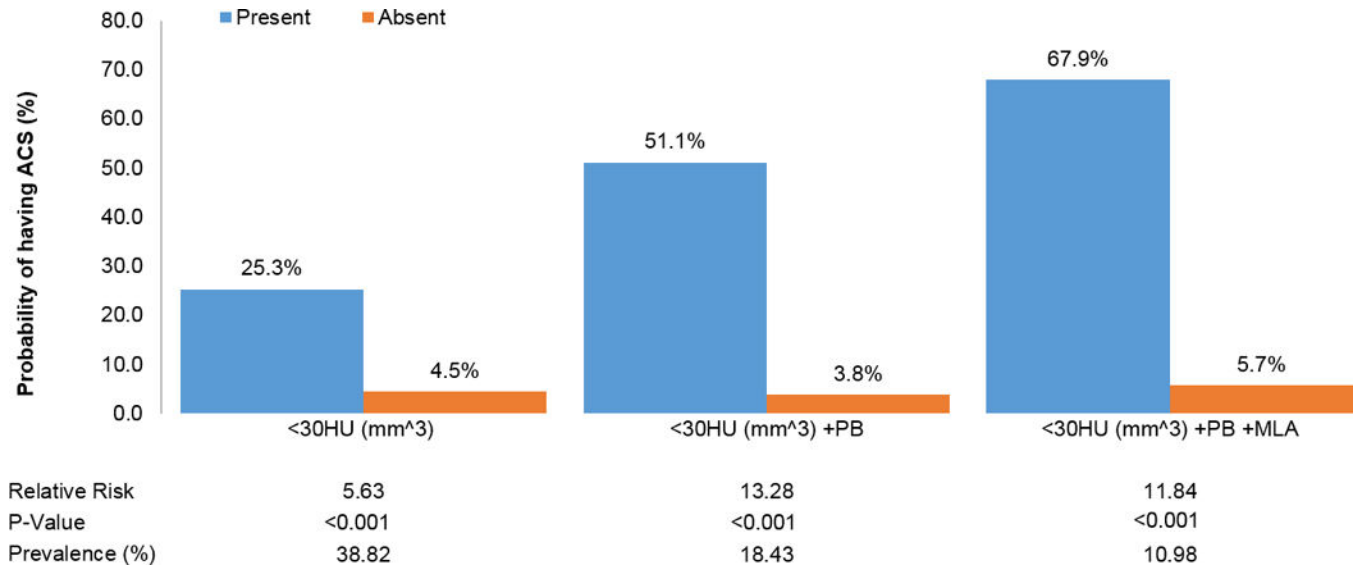

Figure 2. Probability of ACS in patients with high-risk plaque on coronary CTA using IVUS-based definitions for TCFA equivalent (plaque volume <30HU), plaque burden and minimal luminal area

Relative risks for ACS are shown according to presence of IVUS based HRP features. A MLA of 4.0 mm^2 or less and a plaque burden of 70% or more were pre-specified for use in this model, since they have been used frequently in previous studies. For low HU plaque, a prespecified threshold of <30 HU was used as TCFA equivalent, since it corresponds to a necrotic core in IVUS. For the volume of low HU plaque, we used a CTA-specific threshold of 1.31 mm^3, as there is no equivalent definition based on IVUS.

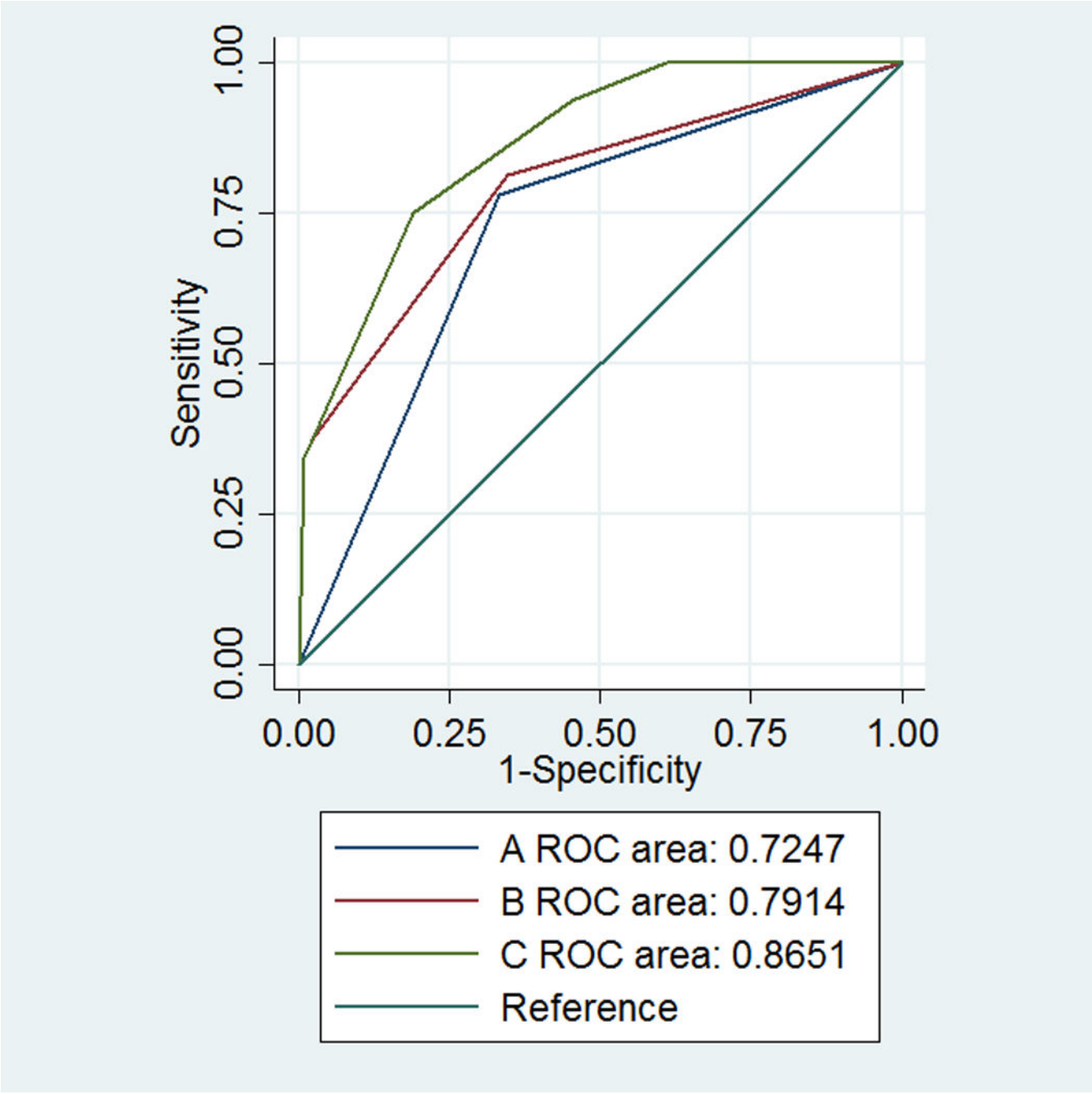

Figure 3.

Receiver operating characteristic curves (ROC) for the prediction of acute coronary syndrome by presence of IVUS based HRP characteristics as measured on coronary CTA: (A) low density plaque (TCFA equivalent), (B) low density plaque (TCFA equivalent) and plaque burden and (C) low density plaque (TCFA equivalent), minimal luminal area and plaque burden. AUC indicates area under the curve (A vs. B: p=0.0082; A vs. C: p=0.0001; B vs. C: p=0.0190)

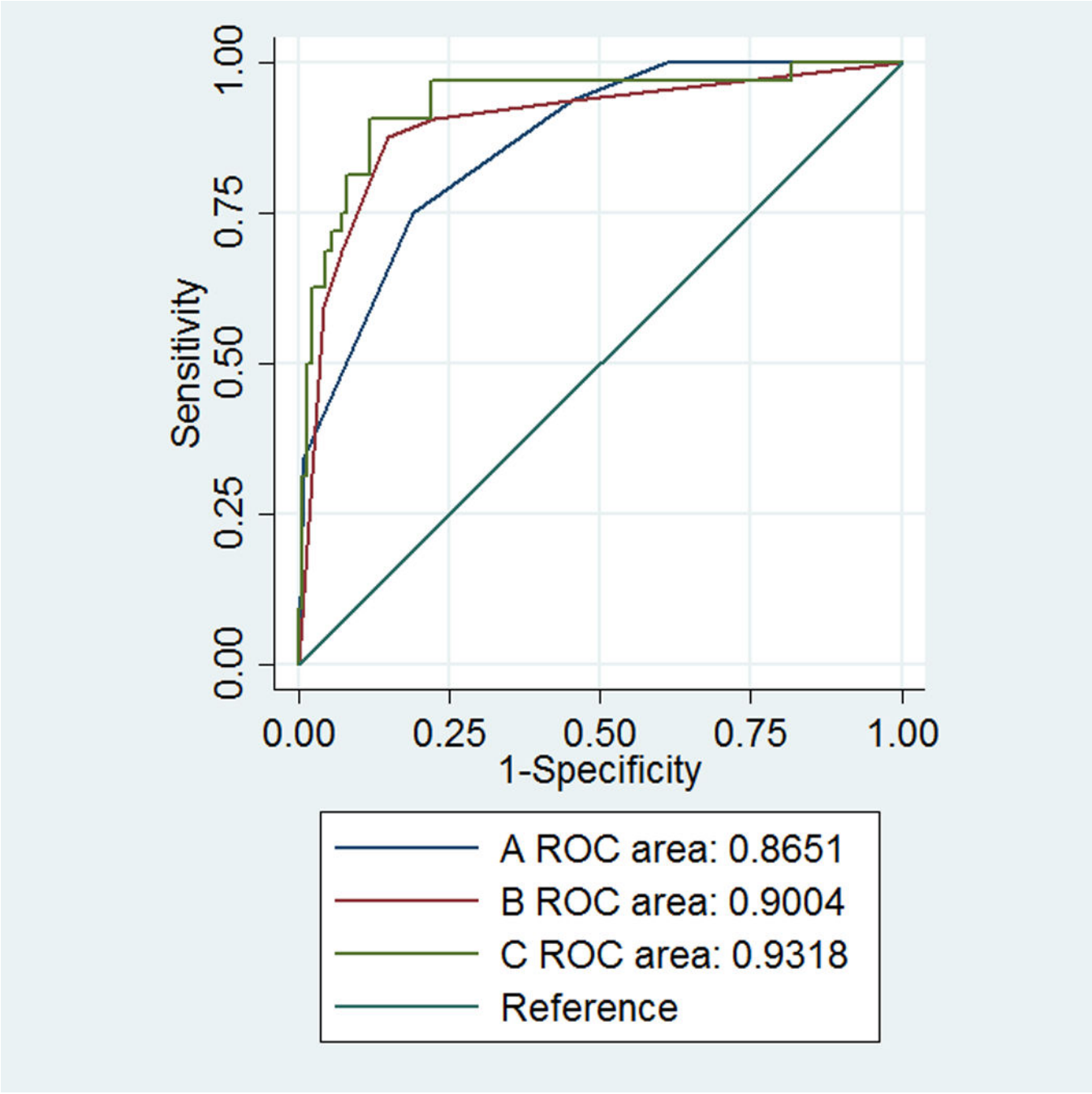

Figure 4.

Receiver operating characteristic curves (ROC) for the prediction of acute coronary syndrome by presence of HRP characteristics (low density plaque (TCFA equivalent), minimal luminal area, plaque burden) using (A) IVUS based and (B) newly derived coronary CTA-specific thresholds, and (C) using all available information from coronary CTA (low density plaque, minimal luminal area, plaque burden, remodeling index, lesion length and

diameter stenosis). AUC indicates area under the curve. (A vs. B: p=0.2347; B vs. C: p=0.0752; A vs. C: p=0.0209)

Table 1

Baseline characteristics of patients with coronary plaque (n=255) stratified by diagnosis of acute coronary syndrome (ACS)

	ACS (n=32)	No ACS (n=223)	p value
Age (years)	57.2 ± 8.5	55.9 ± 7.8	0.428
Male gender, n (%)	26 (81.3)	132 (59.2)	0.019
Cardiovascular risk factors, n (%)			
Hypertension	20 (62.5)	135 (60.5)	1.000
Diabetes mellitus	7 (21.9)	46 (20.6)	0.819
Dyslipidemia	21 (65.6)	117 (52.5)	0.187
Former or current smoker	21 (65.6)	120 (53.8)	0.255
Family history of premature CAD	10 (31.3)	54 (24.2)	0.389
Number of cardiovascular risk factors, n (%)			0.266
0 or 1	7 (21.9)	66 (29.6)	
2 or 3	19 (59.4)	128 (57.4)	
≥ 4	6 (18.8)	29 (13.0)	

ACS = Acute Coronary Syndrome; CAD = Coronary Artery Disease

Table 2

Quantitative coronary plaque measurements of culprit and non-culprit plaque in 32 patients with acute coronary syndrome

	Culprit-Plaque (n=35)	Nonculprit-Plaque (n=172)	p value
	Median (Q1;Q3)	Median (Q1;Q3)	
IVUS-based measures			
Remodeling index	1.19 (0.93-1.35)	1.02 (0.91-1.16)	0.004
Minimal luminal area (mm^2)	0.64 (0.12-3.02)	4.05 (2.17-6.37)	<0.001
Plaque burden (%)	67.1 (55.6-72.1)	48.4 (41.3-56.7)	<0.001
TCFA equivalent – Low HU plaque volume <30 HU (mm^3)	2.34 (0.45-5.61)	0.19 (0.00-1.07)	0.003
Other measures			
Diameter stenosis (%)	65.1 (33.7-83.3)	13.8 (5.3-30.7)	<0.001
Lesion length (mm)	16.5 (8.0-21.1)	7.5 (3.8-13.0)	<0.001

IVUS = Intravascular Ultrasound; Q1;Q3 = 25th percentile, 75th percentile; Remodeling index (calculated as the ratio of the outer vessel wall area at the site of the minimal luminal area and the vessel area defined by the vessel wall reference at that location); Plaque burden (plaque area in % of the total vessel area derived from a cross-sectional view); TCFA = thin cap fibroatheroma; HU = Hounsfield Units; Lesion length (calculated as the centerline distance from the proximal to distal end of the plaque.

Table 3

The results of univariable and multivariable multilevel mixed-effects logistic regression analyses for the prediction of culprit lesions among ACS patients (n=32) (A) and the results of univariable and multivariable logistic regression analyses for the prediction of ACS during index hospitalization among all patients (n=255) (B) using IVUS-based thresholds for the detection of high-risk plaques on coronary CTA.

(A)

	Univariable analysis		Multivariable analysis	
	OR (95%CI)	**p value**	**OR (95%CI)**	**p value**
Remodeling index *	2.04 (0.98-4.26)	0.058	1.11 (0.44-2.78)	0.820
Minimal luminal area (mm^2) *	5.86 (2.17-15.82)	<0.001	2.29 (0.74-7.12)	0.151
Plaque burden (%) *	7.63 (3.02-19.30)	<0.001	3.14 (1.06-9.25)	0.038
TCFA equivalent – Low HU plaque volume <30 HU (mm^3)	11.71 (5.03-27.30)	<0.001	6.60 (2.52-17.24)	<0.001
Lesion length	4.07 (1.87-8.88)	<0.001	2.00 (0.81-4.93)	0.130

(B)

	Univariable analysis		Multivariable analysis	
	OR (95%CI)	**p value**	**OR (95%CI)**	**p value**
Remodeling index *	3.34 (1.32-8.42)	0.011	0.78 (0.25-2.45)	0.673
Minimal luminal area (mm^2) *	18.12 (4.23-77.66)	<0.001	6.82 (1.46-31.79)	0.014
Plaque burden (%) *	26.16 (8.37-81.74)	<0.001	5.71 (1.59-20.58)	0.008
TCFA equivalent – Low HU plaque volume <30 HU (mm^3)	7.19 (2.97-17.39)	<0.001	4.04 (1.46-11.14)	0.007
Lesion length	21.57 (6.36-73.2)	<0.001	7.50 (2.01-27.97)	0.003

* A remodeling index of 1.1 or greater, a MLA of 4.0 mm^2 or less, a plaque burden of 70% and a lesion length of 11.2 mm or greater were pre-specified for use in this model, since they have been used frequently in previous studies. For low HU plaque, a pre-specified HU threshold of <30 HU was used as TCFA equivalent, since it corresponds to a necrotic core in IVUS. For the volume of low HU plaque, we used the newly derived CTA-specific threshold of 1.31 mm^3, as there is no frequently used definition for plaque volume in IVUS.

Table 4

Comparison of discriminatory capacity of quantitative high-risk plaque measurements using IVUS based thresholds and newly derived coronary CTA based thresholds (maximized for AUC) for diagnosis of ACS in patients with coronary plaque (n=255).

	AUC* (95%CI)	p value	NRI (95%CI)**	p value
IVUS based measures				
Remodeling index				
>1.05	0.630 (0.570-0.690)	0.402	0.064 (−0.100-0.227)	0.447
>1.10	0.624 (0.548-0.700)	0.187	0.077 (−0.042-0.196)	0.207
>1.17	**0.662 (0.577-0.747)**			
Minimal luminal area				
≤4mm^2	0.742 (0.689-0.796)	0.066	0.149 (−0.032-0.330)	0.106
≤1.43mm^2	**0.817 (0.736-0.898)**			
Plaque burden				
≥70%	0.676 (0.591-0.762)	<0.001	0.312 (0.060-0.563)	0.015
≥55%	**0.832 (0.768-0.896)**			
TCFA equivalent – Low HU plaque volume <30 HU (mm^3)				
≥1.31 mm^3	**0.725 (0.646-0.804)**			
Other measures				
Diameter stenosis				
≥50%	0.824 (0.741-0.906)	0.317	0.004 (−0.004-0.013)	0.317
≥70%	0.721 (0.632-0.810)	0.005	0.210 (0.047-0.372)	0.011
≥52%	**0.826 (0.743-0.908)**			
Lesion length				
≥11.2mm	0.798 (0.739-0.858)	0.450		
≥13.09mm	**0.817 (0.747-0.886)**			

IVUS = Intravascular Ultrasound;

*AUC = area under the curve (in respect to the dichotomized threshold); 95%CI = 95% confidence interval; Remodeling index (calculated as the ratio of the outer vessel wall area at the site of the minimal luminal area and the vessel area defined by the vessel wall reference at that location); Plaque burden (plaque area in % of the total vessel area derived from a cross-sectional view); TCFA = thin cap fibroatheroma; HU = Hounsfield Units; Lesion length (calculated as the centerline distance from the proximal to distal end of the plaque.

**Improvement of coronary CTA derived thresholds compared to IVUS derived thresholds for the prediction of ACS